Optical, Thermal, Electrical, Damage, and Phase-Matching Properties of Lithium Selenoindate

Jean-Jacques Zondy
Laboratoire Commun de Métrologie LNE-Cnam, 61 rue du Landy, 93210 La Plaine Saint Denis, France,
jean-jacques.zondy@cnam.fr

Valentin Petrov
Max-Born-Institute for Nonlinear Optics and Ultrafast Spectroscopy, 2A Max-Born-Str., D-12489 Berlin, Germany

Ludmila Isaenko and Alexander Yelisseyev
Institute of Geology and Mineralogy, SB RAS, 43 Russkaya Str., 630058 Novosibirsk, Russia

Olivier Bidault
I.C.B., CNRS – Université de Bourgogne, 21078 Dijon, France

Abstract: $LiInSe_2$, a biaxial nonlinear crystal transparent from 0.54 to 10 µm, is successfully grown in large sizes with good optical quality. We summarize all characteristics and physical properties of $LiInSe_2$ essential for nonlinear frequency conversion.

OCIS codes: (160.4330) Nonlinear optical materials; (190.4410) Nonlinear optics, parametric processes.

1. Introduction

To date, only a few suitable nonlinear crystals combining a transparency extending into the mid-IR range above ~5 µm (the upper limit of oxide materials) and large-enough birefringence to permit phase-matching over their transparency ranges are available. All such unary, binary or ternary mid-IR crystals are uniaxial. All of them have their specific advantages but also serious limitations. In the last decade, considerable progress has been made with two orthorhombic (biaxial) ternary chalcogenides, $LiInS_2$ (LIS) and $LiInSe_2$ (LISe). The properties of the sulfide compound LIS were repored in [1]. As a continuation of this work, we performed an extensive characterization study of the related LISe, the results of which will be summarized here, including optical, thermal, electrical, damage, and phase-matching properties, as well as applications in down-conversion nonlinear optical processes.

2. Growth, composition, and structure

LISe is a congruently melting compound that can be grown from the melt using the three elements as starting materials. In the first report on LISe by Negran et al. [2], the crystalline samples grown by directional freezing in graphite crucibles were deep red in color. The yellow LISe phase is closer to the ideal stoichiometric composition.

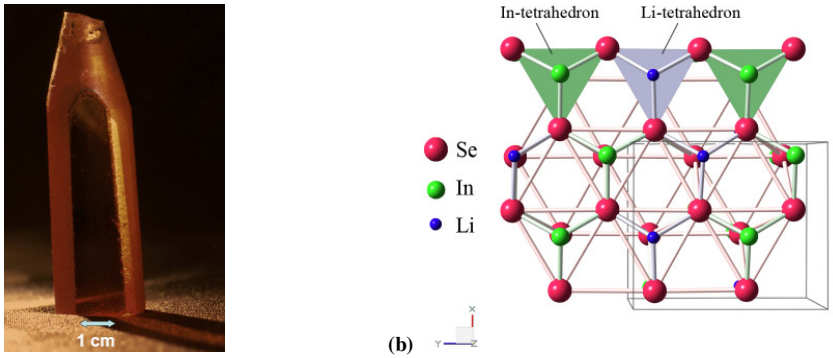

Fig. 1. (a) $LiInSe_2$ boule grown by the Bridgman-Stockbarger technique on oriented seed, annealed in vacuum after growth to improve the transparency and achieve stoichiometry. (b) The orthorhombic unit cell structure of $LiInSe_2$: the box frame gives the orientation of the unit cell.

We use a seeded Bridgman-Stockbarger process in a vertical two-zone furnace with counter pressure to grow large size single-crystal ingots of LISe. In principle, the synthesis and growth of LISe follows the same procedure as that for growing the chalcopyrites $AgGaS_2$ (AGS) and $AgGaSe_2$ (AGSe), except for some refinements related to the volatility of the elements and the chemical reactivity of Li with the container walls. Single crystal ingots obtained can be as large as 30 mm in diameter and 100 mm in length, Fig. 1(a).

The structure of LISe is formed by $LiSe_4$ and $InSe_4$ tetrahedrons, and the Se^{2-} ions are arranged in hexagonal packing with tetragonal and octahedral cavities (tetra- and octapores), Fig. 1(b). The β-$NaFeO_2$ structure is less dense than the chalcopyrite structure of AGS and AGSe due to the presence of these empty cavities in the unit cell.

3. Band-gap, transmission, and vibrational properties

The band-gap of yellow LISe at room temperature is 2.86 eV. The polarization dichroism is weakly pronounced. We performed new polarized measurements of the transmission with state of the art samples of LISe. The measurements indicate that the 50% transmission level extends from 0.54 to 10 μm while the clear transparency range is roughly from 1 to 8 μm. At 1.064 μm the absorption can be as low as 2%/cm. Infrared reflectivity and Raman spectra of LISe are known from the literature and the vibrational modes have been already identified. From absorption features of the transmission spectra and the maximum phonon energy (375 cm^{-1}) it can be concluded that the onset of absorption near 10 μm is due to three-phonon absorption and the cut-off edge is set by two-phonon absorption.

4. Thermal, thermo-optic, and electrical properties

The thermal properties of a nonlinear optical material are crucial in assessing its potential in real nonlinear conversion devices pumped by high power CW or pulsed lasers. Some essential characteristics, such as the specific heat at constant pressure, thermal conductivity, thermal expansion, and thermo-optic coefficients are included in Table I. Temperature and wavelength dependences of some of them will be presented at the conference.

Most of the electrical measurements were performed using a dynamic method under a linear temperature variation. The dc resistivity and the pyroelectric coefficient were deduced by recording the current vs temperature under constant voltage / zero bias. The dielectric response was measured using an impedance analyzer. Some electric characteristics are included in Table I, temperature dependences of the electric permittivity, dielectric losses, resistivity, and pyroelectric coefficients for different crystal orientations will be presented at the conference. Attempts to reverse the polarization by applying a strong dc field (up to 10 kV/cm) failed and the ferroelectric nature of LISe at room temperature phase has not been evidenced.

5. Linear optical and thermo-optic dispersions and phase-matching investigations

The linear optical and thermo-optic dispersion relations allow one to compute accurately the phase-matching directions and temperature tunability. Having in mind the different predictions of the existing Sellmeier equations, we remeasured first the index of refraction of high crystal quality yellow LISe using the technique of minimum angle deviation in the 0.525-12 μm spectral range. New Sellmeier equations were then constructed and refined using phase-matching experimental data. A fitting procedure was also employed to obtain the thermal and wavelength dispersion of the principal thermo-optic coefficients.

We will present analysis of the phase-matching loci of LISe in the *XYZ*-principal optic axes frame. The biaxial phase-matching loci for collinear SHG are categorized using the Hobden classification. This will be illustrated for SHG in LISe at several representative fundamental wavelengths. We will present also precise SHG analysis in the principal planes, including group-velocity-mismatch (spectral acceptance), walk-off angles, and angular acceptance as well as phase-matching properties for sum- and difference-frequency generation (DFG).

6. Nonlinear susceptibility and parametric down-conversion

We determined the elements d_{ij} of the nonlinear tensor from the SHG efficiency in type-I or type-II interactions in the principal planes of LISe and also out of them, see Table I. Analysis of the effective nonlinearity will be presented, in particular for down-conversion of 1064 nm radiation into the mid-IR. We will present also recent experimental results with two frequency down-conversion schemes based on LISe: DFG in the CW regime and nanosecond optical parametric oscillator (OPO) operation. Two tunable (from 700 to 810 nm and from 800 to 900 nm) CW single-frequency Ti:sapphire lasers were used as DFG sources. The tuning range covered in the mid-IR was 5.9-8.1 μm. The net DFG conversion efficiency reached 4.6 $\mu W/W^2$. The nanosecond OPO based on LISe was pumped with 14 ns long pulses at 1064 nm without any signs of two-photon absorption (TPA). Idler tuning between 4.7 and 8.7 μm was achieved. The repetition rate was 100 Hz. Maximum energies of 282 μJ at 6.514 μm and 116 μJ at 8.428 μm were measured. These values correspond to external quantum conversion efficiencies of 10.3% and 4.3%, respectively. The maximum idler average power at 100 Hz amounts to 28 mW, substantially exceeding the level achieved in the literature with AGS (max. 3.7 mW) at similar wavelengths but at lower repetition rate.

7. Laser-induced damage in LISe

Surface damage of LISe was observed on the OPO active elements and studied also with 1 mm thick plates, coated and uncoated. The results of the intracavity/extracavity damage tests at 1064 nm using the same OPO pump will be presented at the conference. Comparing the results with coated and uncoated surfaces one can expect that, for the

present quality of the grown material, optimization of the AR-coating could sustain peak on-axis intensities of about 50 MW/cm^2 or incident pump energy of roughly 40 mJ. We studied also damage caused by CW radiation at 1064 nm and high-power fs-pulses at 820 nm, as well as TPA at 820 nm, see Table I.

Table I. Summary of known crystallographic, optical, thermal and electric properties of LISe.

CRYSTALLOGRAPHIC DATA	
Structure	Wurtzite-type (β-$NaFeO_2$)
Symmetry, point group	Orthorhombic, *mm*2 (negative biaxial)
Space group	$Pna2_1$
Lattice parameters	a≈7.2 Å, b≈8.4 Å, and c≈6.8 Å, Z=4
Principal axes assignment	(X, Y, Z) ↔ (b, a, c)
Density (g/cm^3)	4.47
Microhardness (GPa)	1.75 ± 0.04
OPTICAL PROPERTIES	
Optical transmission	0.54-10 μm (50% level for 10 mm thickness), 0.5-13 μm ("0" level)
Band-gap at 300 K (eV)	2.86
Indices of refraction at 300 K:	
λ=632.8 nm	n_X=2.387, n_Y=2.435, n_Z=2.437
λ=1.064 μm	n_X=2.290, n_Y=2.330, n_Z=2.339
λ=10.6 μm	n_X=2.209, n_Y=2.245, n_Z=2.246
Optical axis angles (0.65 μm < λ < 12 μm)	63°<V_Z<78°
Birefringence walkoff at 1064 nm (mrad)	$\rho_{X\text{-}Y}$=17.3, $\rho_{X\text{-}Z}$=21.2
SHG fundamental wavelength range (nm)	1860-11071
Thermo-optic coefficients (10^{-5}/°C) at 1064 nm, 300 K	dn_X/dT=5.676, dn_Y/dT=9.339, dn_Z/dT=7.368
Absorption coefficient at 1.064 μm (cm^{-1})	2%
Laser damage threshold:	
1064 nm, 10 ns, 10 Hz (GW/cm^2), surface damage	~0.04
820 nm, 220 fs, 1 kHz (GW/cm^2), gray tracks	~55
9.55 μm, 30 ns, single pulse (GW/cm^2)	~0.25
1064 nm, CW (GW/cm^2)	~0.006
Two-photon absorption at 0.82 μm (cm/GW), 220 fs	0.6
Nonlinear optical coefficients (pm/V) at 2.3 μm (fund.)	d_{31}=11.78±5%, d_{24}=8.17±10%, d_{33}=-16±25%
THERMAL PROPERTIES	
Melting point (°C)	915±5
Thermal expansion at 300 K (10^{-5}/K)	α_X=1.76 ±0.18, α_Y=1.1±0.16, α_Z=0.87±0.11
Specific heat at 300 K (J/mol/K)	98.1±1.4
Thermal conductivity at 300 K (W/m/K)	K_X=4.7±0.2, K_Y=4.7±0.2, K_Z=5.5±0.3
ELECTRICAL PROPERTIES	
Pyroelectric coefficient at 300 K (μC/m^{2}K)	16
Pure electro-optic coefficients (relative to $LiInS_2$)	r_{c1}(LISe)≈2.1r_{c1}(LIS), r_{c2}(LISe)≈2.6r_{c2}(LIS)
Electric conductivity 300 K (10^{-12} Ω^{-1}cm^{-1})	σ_X≈3, σ_Y≈0.08, σ_Z≈0.02

8. Conclusion

LISe can now be considered as a mature compound: Among its most relevant advantages over the existing mid-IR crystals, one may quote its excellent thermal stability and high damage threshold suitable for high-power laser applications and its extended phase-matching capabilities (over its entire transparency range) using either type-I or type-II interactions in or out of principal planes. Such an extended phase-matching capability is still compatible with low birefringence walk-off angles. LISe exhibits effective nonlinearity higher than that of the related LIS and comparable to that of AGS. Taking into account its similar transparency range, LISe is a good candidate for 1.064 μm pumped mid-IR OPOs with the advantages of higher thermal conductivity and damage threshold. With respect to AGS(e) ternary chalcopyrite materials, LISe displays a nearly isotropic thermal expansion behavior with 3 to 5-times-larger thermal conductivities associated with high optical damage thresholds, and low intensity-dependent absorption, allowing direct high-power down-conversion from the near-IR, especially 1064 nm, to the deep mid-IR.

References:

1. S. Fossier, S. Salaün, J. Mangin, O. Bidault, I. Thenot, J.-J, Zondy, W. Chen, F. Rotermund, V. Petrov, P. Petrov, J. Henningsen, A. Yelisseyev, L. Isaenko, S. Lobanov, O. Balachninaite, G. Slekys, V. Sirutkaitis, "Optical, vibrational, thermal, electrical, damage and phase-matching properties of lithium thioindate", J. Opt. Soc. Am B **21**, 1981-2007 (2004).
2. T. J. Negran, H. M. Kasper, A. M. Glass, „Pyroelectric and electrooptic effects in $LiInS_2$ and $LiInSe_2$", Mat. Res. Bull. **8**, 743-748 (1973).